

γ rays, and is therefore much less certain in the low-frequency region. These spectra are shown in Fig. 2 for the different systems considered, together with values deduced using the centroid method. Much of the detailed structure of the $\mathfrak{F}_{\text{eff}}^{(2)}$ spectrum is lost in the $\mathfrak{F}_{\text{eff}}^{(1)}$ spectrum. The increase at low frequencies is due both to the Coriolis antipairing and to the first backbend. The values deduced from the centroid method are systematically higher by 5 to 10%. Part of this can be accounted for by systematic effects in this method due to the narrowing of the difference spectra with increasing spin. It might also be partly associated with temperature effects, since the centroid method always involves the very first transitions emitted, and therefore states at higher temperatures.

The determination of dynamic effective moments of inertia to much higher frequencies provides some new insights into nuclear behavior at very high spins. The observed values at high spins are very large, approaching twice the rigid-sphere value. The evidence suggests that these are due largely to alignment of proton orbitals, probably $i_{13/2}$ and $h_{9/2}$. The observed features would be consistent with increasing triaxiality at these spins ($50\hbar - 55\hbar$) although other possibilities certainly exist.

This work was supported by the Director, Office of Energy Research, Division of Nuclear Physics of the Office of High Energy and Nuclear Physics of the U. S. Department of Energy under Contract No. DE-AC03-76SF00098.

^(a)Permanent address: Physik Department, Technische Universität, München, West Germany.

^(b)Permanent address: Hahn-Meitner-Institute Berlin, D-1000 Berlin 38, West Germany.

^(c)Permanent address: Comisión Nacional de Energía Atómica, Buenos Aires, Argentina.

^(d)Permanent address: C.S.T.N., B.P. 1017, Alger, Algeria.

¹A. Bohr and B. Mottelson, Phys. Scr. 24, 71 (1981).

²Except when numerical values are involved, we use units where $\hbar = 1$.

³M. A. Deleplanque *et al.*, Phys. Rev. Lett. 45, 172 (1980).

⁴H. J. Körner *et al.*, Phys. Rev. Lett. 43, 490 (1979).

⁵M. A. Deleplanque, I. Y. Lee, F. S. Stephens, R. M. Diamond, and M. M. Leonard, Phys. Rev. Lett. 40, 629 (1978).

⁶Th. Dössing, private communication.

⁷G. Leander, Y. S. Chen, and B. S. Nilsson, Phys. Scr. 24, 164 (1981).

⁸S. Frauendorf, Phys. Scr. 24, 349 (1981).

⁹M. A. Deleplanque, Phys. Scr. 24, 158 (1981).

Measurement of the ${}^7\text{Be}(p, \gamma){}^8\text{B}$ Reaction Cross Section at Low Energies

B. W. Filippone,^(a) A. J. Elwyn, and C. N. Davids
Argonne National Laboratory, Argonne, Illinois 60439

and

D. D. Koetke
Valparaiso University, Valparaiso, Indiana 46383

(Received 4 November 1982)

The absolute total cross section for the reaction ${}^7\text{Be}(p, \gamma){}^8\text{B}$ has been measured for $E_{\text{c.m.}} = 117 - 1230$ keV by detecting the delayed α particles following the ${}^8\text{B}$ β decay. Two independent methods have been used to determine the areal density of the ${}^7\text{Be}$ target. The inferred zero-energy S factor from the present experiment is $S_{17}(0) = 0.0216 \pm 0.0025$ keV b. This value reduces the predicted ${}^{37}\text{Cl}$ solar-neutrino capture rate by $\sim 25\%$.

PACS numbers: 25.40.Lw, 27.20.+n

In the solar interior ${}^8\text{B}$ is thought to be produced via the reaction ${}^7\text{Be}(p, \gamma){}^8\text{B}$. The subsequent β decay of this ${}^8\text{B}$ gives a spectrum of neutrinos with $E_\nu = 0 - 14$ MeV. These neutrinos are expected to provide $\sim 75\%$ of the events in the

Brookhaven National Laboratory ${}^{37}\text{Cl}$ solar-neutrino experiment.¹ The discrepancy between the calculation of the solar-neutrino flux^{2,3} and the experiment persists (the so-called solar-neutrino problem). It has been noted recently² that a sig-

nificant portion (or perhaps all) of this discrepancy may be due to a lack of accurate experimental input to the calculations. A key part of this input is the measured cross sections for the nuclear reactions involved in the proton-proton chain.

Of the previous measurements⁴⁻⁸ of the ${}^7\text{Be}(p, \gamma){}^8\text{B}$ cross section at low energies, only two^{5,6} have been used in the most recent evaluation³ of the cross-section factor,

$$S(E_{c,m.}) = \sigma E_{c,m.} \exp(E_G/E_{c,m.})^{1/2}, \quad (1)$$

where E_G is the Gamow energy [$E_G = (2\pi\alpha Z_1 Z_2)^2 \times \mu c^2/2$; μ is the reduced mass of the incident channel, α is the fine-structure constant]. Furthermore, there are inconsistencies in the value of the ${}^7\text{Li}(d, p){}^8\text{Li}$ cross section which is used for normalization of all but one⁸ of the previous experiments. Two recent measurements^{9,10} of this cross section, while in agreement with each other, are 10–30% lower than most previously published experimental values.¹¹

In this Letter we report new measurements of the ${}^7\text{Be}(p, \gamma){}^8\text{B}$ cross section and the resulting S factors down to $E_{c,m.} = 117$ keV, with emphasis on numerous consistency checks to reduce possible systematic errors. The cross section was measured by detecting the delayed α particles from the sequence ${}^7\text{Be}(p, \gamma){}^8\text{B} \rightarrow {}^8\text{Be}^* \rightarrow 2\alpha$. The experiment was performed at the Argonne National Laboratory Dynamitron accelerator with essentially the same apparatus as was used in Ref. 10. Briefly, the target was mounted on a rotating arm which was transferred in vacuum from a bombardment chamber to a counting chamber where the α particles from the ${}^8\text{B}$ decay ($t_{1/2} = 0.77$ sec) were detected. A silicon surface-barrier detector with a 300-mm² active area and a 23- μm depletion depth was installed to detect the α particles. A thin detector is necessary to reduce the background from the high flux of 478-keV γ rays from the ${}^7\text{Be}$ decay ($\sim 3 \times 10^8$ γ/sec). In addition, large-area cold traps were employed to provide a chamber pressure $\leq 5 \times 10^{-7}$ Torr and to help reduce carbon buildup on the target.

The target consisted of 81.2 ± 6.0 mCi of ${}^7\text{Be}$ [produced via the ${}^7\text{Li}(p, n){}^7\text{Be}$ reaction at the Argonne Dynamitron] electrodeposited on a 0.25-mm-thick Pt disk in a (4.95 ± 0.13) -mm-diam circle. Following the deposition the Pt disk was flamed red hot in air for several minutes to give the final target of beryllium oxide. Details of the target preparation will be published elsewhere.¹²

For the determination of the cross section the

product of ${}^7\text{Be}$ areal density and detector solid angle is required and in the present experiment this quantity was determined by two independent methods. In the first, the product was determined directly by monitoring the buildup of ${}^7\text{Li}$ which is produced in the decay of the unstable target nucleus ${}^7\text{Be}$ ($t_{1/2} = 53.3$ d, e^- capture decay with a 10.35% branch to the 478-keV excited state in ${}^7\text{Li}$). This was accomplished by measuring the α -particle yield from the reaction sequence ${}^7\text{Li}(d, p){}^8\text{Li} \rightarrow {}^8\text{Be} \rightarrow 2\alpha$ at the 0.77-MeV resonance in ${}^9\text{Be}$ as a function of time; i.e., as the ${}^7\text{Be}$ decays, ${}^7\text{Li}$ is built up and the yield of ${}^8\text{Li}$ in the (d, p) reaction increases. These measurements were performed before, during, and after the ${}^7\text{Be}(p, \gamma){}^8\text{B}$ experiment. This procedure yielded a product of initial ${}^7\text{Be}$ areal density and solid-angle fraction ($\Omega/4\pi$) of $(2.24 \pm 0.19) \times 10^{16}$ atoms/cm², with use of a value of 157 ± 13 mb for the ${}^7\text{Li}(d, p){}^8\text{Li}$ peak cross section which was determined from an analysis of all the previous data.¹³ In the second method a NaI(Tl) detector in conjunction with 10-cm-thick Pb collimators of 0.5 and 1.3 mm diam were used to scan the γ -ray activity of the target. From these scans the uncertainty in the areal density due to non-uniformities in the target was found to be $\pm 5\%$. This technique yielded an effective target diameter which, when combined with activity measurements using standard calibrated γ -ray sources, allowed the determination of the ${}^7\text{Be}$ areal density. The solid angle of the α detector was determined to be $(23.1 \pm 1.5)\%$ of 4π . The product of the separately determined ${}^7\text{Be}$ areal density and solid-angle fraction was $(2.40 \pm 0.27) \times 10^{16}$ atoms/cm², in good agreement with the value extracted by using the (d, p) cross section discussed above. An average of these two independent measurements was used to obtain the final ${}^7\text{Be}(p, \gamma){}^8\text{B}$ cross sections.

Integration of the beam and control of the timing cycle are described in Ref. 10. A series of collimators provided a beam spot of 3.2 mm diam. The Dynamitron energy scale was calibrated by use of resonances in the reaction ${}^{19}\text{F}(p, \alpha\gamma){}^{16}\text{O}$ at 224.4, 340.46, and 872.11-keV bombarding energy. Energy loss of the beam from carbon buildup on the target (~ 3 keV) and through the target itself (~ 15 keV) was determined from periodic measurements of the shape of the ${}^7\text{Li}(p, \gamma){}^8\text{Be}$ resonance at 441.1 keV, taken during the course of the ${}^7\text{Be}(p, \gamma){}^8\text{B}$ experiment.

The spectrum of α particles is shown in Fig. 1 for $E_{c,m.} = 117$ and 632 keV. The background due

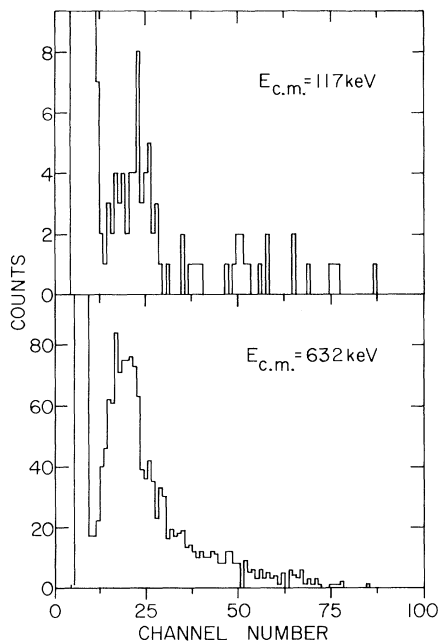


FIG. 1. Delayed α -particle spectra from the reaction sequence ${}^7\text{Be}(p, \gamma){}^8\text{B} \rightarrow {}^8\text{Be}^* \rightarrow 2\alpha$. The data have been compressed by a factor of 4 by summing adjacent channels. The shape of each spectrum is influenced by experimental factors such as detector thickness, target-detector geometry, ${}^8\text{B}$ recoil energy, and total acquisition time (which affects the background level).

to the 478-keV γ rays from ${}^7\text{Be}$ decay can be seen at low energy; the cutoff at channel 5 is an instrumental effect. Of the various possible backgrounds contributing to the α -particle yields (beam-on, beam-off, and deuteron contamination of the proton beam), that associated with cosmic rays and natural radioactivity in the detector and the chamber was by far the largest. This background ranged from $\leq 1\%$ of the integrated yield at the high energies to 15% of the yield at the lowest energy.

The experimental results are shown in Fig. 2. The cross sections were obtained from the integrated α -particle yields in a manner similar to that described in Ref. 10. The average energy of the beam has been calculated from the energy loss in the front carbon layer and in the target. The lowest-energy point (117 keV) was obtained with an H_2^+ beam. Calculations¹³ indicated that effects due to breakup of the molecular ion (Coulomb explosion) were less than 1%. A potentially much larger correction to the α -particle yield is the background due to deuteron (D^+) contamination of the H_2^+ beam. However, because of the low beam energy, this background was found to be

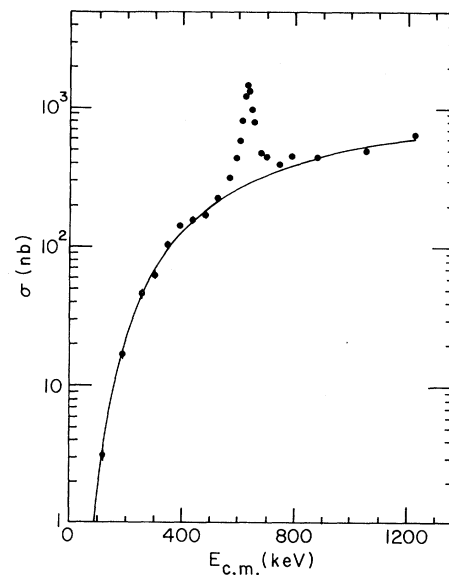


FIG. 2. Total cross section for the reaction ${}^7\text{Be}(p, \gamma){}^8\text{B}$ as a function of the center-of-mass energy. The solid curve is the cross section calculated from the theoretical S factors of Ref. 14 normalized to the data. If not shown the error bars (statistical only) are smaller than the data points.

only $\sim 2\%$ of the yield, as measured with the H_2^+ beam bombarding a thick ${}^7\text{LiF}$ target.

Figure 3 gives the S factors derived from Eq. (1). The smooth curve represents a best least-

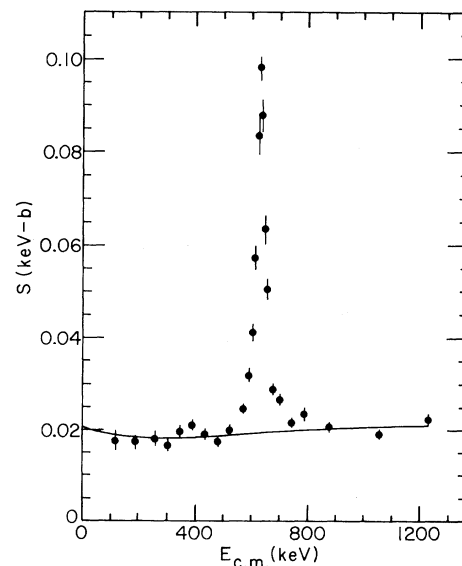


FIG. 3. ${}^7\text{Be}(p, \gamma){}^8\text{B}$ S factor vs center-of-mass energy. The solid curve is a least-squares normalization of the calculation of Ref. 14 to the off-resonance data.

TABLE I. Zero-energy S factor for ${}^7\text{Be}(p, \gamma){}^8\text{B}$ obtained by normalizing the calculation of Ref. 14 to the various experiments. A value of 157 mb (Ref. 13) for the peak of the ${}^7\text{Li}(d, p){}^8\text{Li}$ cross section ($E_d \approx 0.77$ MeV) has been used where indicated.

Reference	$S_{17}(0)$ (keV b)
4 ^a	0.016 ± 0.006
5 ^a	0.028 ± 0.003
6 ^a	0.0273 ± 0.0024
7 ^a	0.0214 ± 0.0022
8 ^b	0.045 ± 0.011
Present ^a	0.0221 ± 0.0028^c
Present ^b	0.0206 ± 0.0030^c

^a ${}^7\text{Be}$ areal density determined from the ${}^7\text{Li}(d, p){}^8\text{Li}$ cross section.

^b ${}^7\text{Be}$ areal density determined from γ -ray activity.

^cThese uncertainties are not completely independent. This fact is reflected in the total uncertainty for $S_{17}(0)$ given in the text.

squares normalization of the calculation of Tombrello¹⁴ to the off-resonance data. This gives an extrapolated zero-energy S factor $S_{17}(0) = 0.0216 \pm 0.0025$ keV b (where the error includes both statistical and systematic uncertainties), 25–35% lower than the values used in recent solar-model calculations^{2, 3, 15} which range from 0.029 to 0.033 keV b. It should be emphasized that these S factors were based only on cross sections normalized to measured ${}^7\text{Li}(d, p){}^8\text{Li}$ values. The present value, as discussed above, utilized two methods for the determination of the ${}^7\text{Be}$ areal density, one of which is independent of the value of the ${}^7\text{Li}(d, p){}^8\text{Li}$ peak cross section. In this connection we note that the results of the two methods are in excellent agreement with one another when the ${}^7\text{Li}(d, p){}^8\text{Li}$ cross sections of Refs. 9 and 10 are utilized. Reasonable agreement between the two techniques is also obtained for all previously measured ${}^7\text{Li}(d, p){}^8\text{Li}$ cross sections except those of Refs. 5 and 16. A summary of the experimental values for $S_{17}(0)$ are shown in Table I. The measurements which rely on the ${}^7\text{Li}(d, p){}^8\text{Li}$ cross section have been normalized to a cross section of 157 mb for comparison. Aside from the high value of Ref. 8 there is fair agreement between the data. A detailed discussion of these values and a more complete report of the present experiment is currently in preparation.¹³

On the basis of the calculation of the dependence of the solar-neutrino capture rate on S_{17} discussed in Ref. 10, the present value for $S_{17}(0)$ leads to a predicted ${}^{37}\text{Cl}$ neutrino capture rate of

5.3 SNU (1 SNU $\equiv 10^{-36}$ ν captures per target atom per second), a reduction of ~ 2 SNU from recent predictions of 7–8 SNU.^{2, 3} A weighted average of the values of Table I [$\bar{S}_{17}(0) = 0.0238 \pm 0.0023$ keV b] gives a ${}^{37}\text{Cl}$ capture rate of 5.6 SNU. Since the latest value of the measured capture rate is 2.1 ± 0.3 SNU,¹ the present results provide at least a partial solution to the solar-neutrino problem.

It is a pleasure to thank R. Evans, M. Finn, W. Ray, Jr., M. Wahlgren, and the Dynamitron staff for assistance with the experiment. We would also like to acknowledge helpful discussions with J. Schiffer and R. Armani. This work was supported by the U. S. Department of Energy under Contract No. W-31-109-Eng-38.

^(a)Also at the Department of Physics, The University of Chicago, Chicago, Ill. 60637.

¹R. Davis, Jr., in Proceedings of the Informal Conference on Status and Future of Solar Neutrino Research, Brookhaven National Laboratory, Upton, New York, 1978, edited by G. Friedlander, BNL Report No. BNL 50879 (unpublished), Vol. 1, p. 1; B. T. Cleveland, R. Davis, Jr., and J. K. Rowley, in *Proceedings of the 1980 International DUMAND Symposium*, edited by V. J. Stenger (Hawaii Deep Underwater Muon and Neutrino Detector Center, Honolulu, Hawaii, 1981), Vol. 2, p. 111.

²B. W. Filippone and D. N. Schramm, *Astrophys. J.* **253**, 393 (1982).

³J. N. Bahcall, W. F. Huebner, S. H. Lubow, P. D. Parker, and R. K. Ulrich, *Rev. Mod. Phys.* **54**, 767 (1982).

⁴R. W. Kavanagh, *Nucl. Phys.* **15**, 411 (1960); R. W. Kavanagh, in *Essays in Nuclear Astrophysics*, edited by C. A. Barnes, D. D. Clayton, and D. N. Schramm (Cambridge Univ. Press, Cambridge, England, 1982), p. 159.

⁵P. D. Parker, *Phys. Rev.* **150**, 851 (1966), and *Astrophys. J.* **153**, L85 (1968).

⁶R. W. Kavanagh, T. A. Tombrello, J. M. Mosher, and D. R. Goosman, *Bull. Am. Phys. Soc.* **14**, 1209 (1969); R. W. Kavanagh, in *Cosmology, Fusion and Other Matters*, edited by F. Reines (Colorado Associated Univ. Press, Boulder, 1972), p. 169.

⁷F. J. Vaughn, R. A. Chalmers, D. Kohler, and L. F. Chase, Jr., *Phys. Rev. C* **2**, 1657 (1970).

⁸C. Wiezorek, H. Kräwinkel, R. Santo, and L. Wallek, *Z. Phys. A* **282**, 121 (1977). In this experiment the ${}^7\text{Be}$ areal density was determined by mapping out the γ -ray activity from the target, but the cross section was determined at only one energy ($E_p = 360$) and with a large ($\pm 25\%$) uncertainty.

⁹A. J. Elwyn, R. E. Holland, C. N. Davids, and W. Ray, Jr., *Phys. Rev. C* **25**, 2168 (1982).

¹⁰B. W. Filippone, A. J. Elwyn, W. Ray, Jr., and D. D. Koetke, *Phys. Rev. C* **25**, 2174 (1982).

¹¹See Ref. 10 for a complete discussion of experimental values.

¹²B. W. Filippone and M. Wahlgren to be published.

¹³B. W. Filippone, A. J. Elwyn, C. N. Davids, and D. D. Koetke, to be published.

¹⁴T. A. Tombrello, Nucl. Phys. 71, 459 (1965). Similar results, including the upturn in S_{17} near zero energy, have been obtained in more recent calculations [R. G. H. Robertson, Phys. Rev. C 7, 543 (1973); F. C.

Barker, Aust. J. Phys. 33, 177 (1980), private communication].

¹⁵J. N. Bahcall, S. H. Lubow, W. F. Huebner, N. H. Magee, Jr., A. L. Merts, M. F. Argo, P. D. Parker, B. Rozsnayi, and R. K. Ulrich, Phys. Rev. Lett. 45, 945 (1980).

¹⁶A. E. Shilling, N. F. Mangelson, K. L. Nielson, D. R. Dixon, M. W. Hill, G. L. Jensen, and V. C. Rogers, Nucl. Phys. A263, 289 (1976).